Preprints of the 21st IFAC World Congress (Virtual)
Berlin, Germany, July 12-17, 2020

Angle-based Formation Shape Control with Velocity Alignment*

Liangming Chen [*,**] **Ming Cao** [*] **Zhiyong Sun** [***]
Brian D. O. Anderson [****] **Chuanjiang Li** [**]

[*] *Faculty of Science and Engineering, University of Groningen, Groningen, 9747 AG, The Netherlands. (e-mail: l.m.chen@rug.nl, m.cao@rug.nl).*
[**] *Department of Control Science and Engineering, Harbin Institute of Technology, Harbin, 150001, China. (e-mail: lichuan@hit.edu.cn).*
[***] *Department of Electrical Engineering, Eindhoven University of Technology (TU/e), the Netherlands. (e-mail: sun.zhiyong.cn@gmail.com).*
[****] *Hangzhou Dianzi University, Hangzhou 310018, China, also with the Research School of Electrical, Energy and Material Engineering, Australian National University, Acton ACT 2601, Australia, and also with Data61-CSIRO, Acton ACT 2601, Australia. (e-mail: brian.anderson@anu.edu.cn).*

Abstract: With the rapid development of sensor technology, bearing/angle measurements are becoming cheaper and more reliable, which motivates the study of angle-based formation shape control. This work studies how to achieve angle-based formation control and velocity alignment at the same time, in which all agents can form a desired angle-rigid formation and translate with the same velocity simultaneously. The agents' communication topology for the achievement of velocity alignment is described by a connected graph, while the formation shape is determined by a set of angles that are associated with triangles within the formation and computed using bearing measurements. A simulation example validates the effectiveness of the theoretical results.

Keywords: Multi-agent systems, formation control, angle rigid formation, velocity alignment.

1. INTRODUCTION

Multi-agent distributed control has been widely studied recently in the community of systems and control, and one of the fundamental problems is formation control Anderson et al. (2008); Oh et al. (2015), etc. For the formation control problem, different approaches have been proposed under different formation shape descriptions and applicable measurements, e.g., relative positions, distances, bearings, and angles, see e.g., Oh et al. (2015); Anderson et al. (2008); Zhao and Zelazo (2019); Ahn (2019). For a formation shape described by relative positions, the formation control algorithms presented in Oh and Ahn (2014) require all agents' coordinate frames to be exactly aligned, i.e., the orientations of all agents' coordinate frames should be the same. Relaxing the requirement on the alignment of coordinate frames, formation control algorithms are designed in Krick et al. (2009) which employ distances for the formation shape description and use local relative positions as the measurements. Recently, with the aid of rapid development in sensor technology, vision-based sensors can be used to produce bearing/angle information Zhao and Zelazo (2019); Jing et al. (2019). These developments enable applications of the bearing rigidity and bearing-only formation control algorithms Zhao and Zelazo (2016). By employing interior angles as the formation shape description and local bearings as the measurements, a triangular formation control algorithm is designed in Basiri et al. (2010). Further in Chen et al. (2019), the extension of Basiri et al. (2010) to arbitrary number of agents under a special set of angle constraints is studied. However, none of the agents' moving velocities are controlled in Basiri et al. (2010); Chen et al. (2019), and in both cases a stationary formation is asymptotically obtained. As such, the obtained stationary formations fall short of what is required in practical situations, e.g., formation flying of fixed wing aircraft. To attain a nonzero velocity, the works in Deghat et al. (2018) and Deghat et al. (2016) combine distance-based formation shape control and velocity alignment for single- and double-integrator systems, respectively, in which the use of angle or bearing measurements is not addressed.

Motivated by the advantages of bearing measurements and the practical requirements of securing nonzero velocity, the goal of this paper is to design a control algorithm such that a group of agents can achieve the desired angle rigid formation and move with the same velocity simultaneously. The characteristics of the proposed control algorithm include the following: (1) For the designed control algorithm, bearing measurements are needed, while neither distance information nor relative position measurements are required. (2) Asymptotically, all agents will achieve the desired angle-described formation shape and move with the same non-zero velocity. (3) The formation shape is free up to scaling, as well as overall orientation and location of

* The work of Chen and Li was supported in part by the National Natural Science Foundation of China (Grant No. 61876050, 61673135). The work of Anderson was supported by the Australian Research Council's Discovery Project under Grant DP-160104500 and Grant DP-190100887.

centroid. (4) The common alignment velocity is not determined by a leader, but evolves essentially as a consensus value.

2. PRELIMINARIES AND PROBLEM FORMULATION

In this section, we introduce the basic preliminaries, including relevant graph theory, bearing measurements, and the concept of an angle rigid formation. Then the research problem is formally formulated.

2.1 Graph theory

Let $\mathcal{G}(\mathcal{V},\mathcal{E})$ be an undirected graph describing the communication topology between pairs of agents. Here, $\mathcal{V}=\{1,\cdots,N\}$ is the vertex set with N vertices, each of which corresponds to one agent, and $\mathcal{E}\subset\mathcal{V}\times\mathcal{V}$ is the edge set, where $(i,j)\in\mathcal{E}$ if agents i and j can communicate with each other. Agent i's neighbor set $\mathcal{N}_i$ denotes the set of all the agents that can communicate with agent i. Let $\mathcal{L}=[L_{ij}]$ be the Laplacian matrix associated with $\mathcal{G}$, in which for $i\neq j$, $L_{ij}=-1$ if there is an edge between j and i, and $L_{ij}=0$ otherwise, and $L_{ii}=-\sum_{j=1}^{N}L_{ij}$. A path between nodes v_{i_1} and v_{i_s} is a sequence of edges $(v_{i_1},v_{i_2}),(v_{i_2},v_{i_3}),...,(v_{i_{s-1}},v_{i_s})$ with distinct nodes $v_{i_k},k=1,...,s$. A graph is said to be connected if for each pair of distinct vertices v_i and v_j, there is a path between them. Now, we adopt the following common assumption

Assumption 1. The communication graph $\mathcal{G}$ is connected.

Lemma 1. Ren and Beard (2008) If Assumption 1 holds, then $\lambda_1(\mathcal{L})=0<\lambda_2(\mathcal{L})\leq\cdots\leq\lambda_N(\mathcal{L})$, where $\lambda_i(\mathcal{L})$ denotes the ith real eigenvalue of the matrix $\mathcal{L}$ with an ascending order.

2.2 Bearing measurements

Agent i measures the bearing $\phi_{ij}\in[0,2\pi),j\in\bar{\mathcal{N}}_i$ towards agent j evaluated counter-clockwise from agent i's local X-axis; here $\bar{\mathcal{N}}_i$ denotes the set of all the agents to which agent i can measure the bearing. For a triangular formation, $\bar{\mathcal{N}}_i=\{(i+1)\bmod 3,(i-1)\bmod 3\}\in\{1,2,3\}$, and $\phi_{i(i+1)}=\phi_{31}$ when $i=3$, $\phi_{i(i-1)}=\phi_{13}$ when $i=1$. First, we introduce the auxiliary angle

$$\theta_i=|\phi_{i(i+1)}-\phi_{i(i-1)}|\in[0,2\pi), \tag{1}$$

which is the angle measured counter-clockwise from $\min\{\phi_{i(i+1)},\phi_{i(i-1)}\}$ to $\max\{\phi_{i(i+1)},\phi_{i(i-1)}\}$ with respect to agent i's local X-axis. Then, we define the interior angle α_i to be

$$\measuredangle(i-1)i(i+1)=\alpha_i=\begin{cases}\theta_i, \text{ if } \theta_i\leq\pi\\ 2\pi-\theta_i, \text{ otherwise}\end{cases} \tag{2}$$

where $\alpha_i\in[0,\pi]$ represents agent i's interior angle in the triangle $(i-1)i(i+1)$, see Fig. 1.

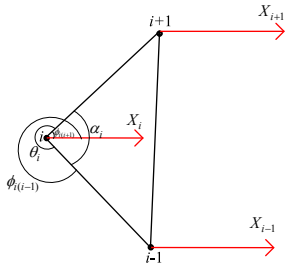

Fig. 1. The bearing measurements.

2.3 Angle rigid formation

Different from the formation described by displacements, distances and/or bearings, the formation in this work is described by a set of triple-agent angles. To guarantee that the desired formation is unique under the given angle constraints (up to scaling, translation and rotation), the formation is required to be *angle rigid*. In the following, we briefly introduce how to construct an angle rigid formation by building it up through a series of steps which add one vertex at a time to an already angle rigid structure. The construction is similar to a sequence of Henneberg vertex addition steps, see e.g. Tay and Whiteley (1985); for more details about angle rigidity, we refer the readers to Chen et al. (2019).

To construct an angle rigid formation, we first define an angle set $\mathcal{A}\subset\mathcal{V}\times\mathcal{V}\times\mathcal{V}$ corresponding to the angle constraints, where each member of $\mathcal{A}$ has three ordered vertices. Certain orderings of certain sets $\mathcal{A}$ then allow the recursive construction of the formation, in the following way.

Step 1: The first three entries of $\mathcal{A}$ correspond to three interior angles of a triangle with vertices 1, 2 and 3, the angles being $\measuredangle 312,123,231$. Using these three values one constructs the first triangular formation $\triangle 123$ by three interior angles $\measuredangle 312,\measuredangle 123,\measuredangle 231$. The scale is free (and actually determines the scale of the whole formation).

Step 2: One adds vertex 4 to the formation. This requires knowledge of the next two elements of $\mathcal{A}$, which must be one of the following three possibilities: 142 and 243, 142 and 143, or 243 and 143. Note that 4 is the vertex at which angles subtended by two other vertices are measured. For example, in Fig. 2, point 4 is merged by adding two angle constraints: $\measuredangle 142$, $\measuredangle 243$.

...

Step $k-2$: Merging point k by adding two angle constraints of the form: $\measuredangle j_1kj_2$ and $\measuredangle j_2kj_3$, $j_1,j_2,j_3\in\{1,...,k-1\},j_1\neq j_2\neq j_3$.

...

Step $N-2$: Merging point N by adding two angle constraints: $\measuredangle i_1Ni_2$ and $\measuredangle i_2Ni_3$, $i_1,i_2,i_3\in\{1,...,N-1\},i_1\neq i_2\neq i_3$.

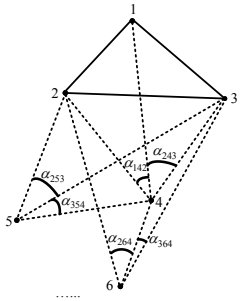

Fig. 2. Formation construction staring from a triangular shape.

According to the above $(N-2)$ steps, the angle set can be written into $\mathcal{A}=\{(3,1,2),(1,2,3),(2,3,1),(1,4,2),(2,4,3),\cdots,(j_1,k,j_2),(j_2,k,j_3),\cdots,(i_1,N,i_2),(i_2,N,i_3)\}$. According to the Type-1 vertex addition in Chen et al. (2019) and (Chen et al., 2019, Proposition 2), one has that the above constructed formation is angle rigid. To guarantee the uniqueness of each merging point in Steps 2 to $(N-2)$ or global angle rigidity of the formation, the following assumption is given.

Assumption 2. In each merging step, the new adding point i under the two angle constraints j_1ij_2 and j_2ij_3 is unique.

Remark 1. Note that the uniqueness in Assumption 2 can always be guaranteed by using signed angles $\measuredangle jik \in [0, 2\pi)$ because each signed angle constraint represents an arc and two arcs with one common starting point have at most one intersection; see (Chen et al., 2019, Proposition 2). Because only local stability is considered in this work, we still use $\measuredangle jik \in (0, \pi)$ in the following analysis.

2.4 Problem formulation

Consider all agents moving in the plane, and each agent is governed by the following single-integrator dynamics

$$\dot{p}_i = u_i, \tag{3}$$

where i represents the ith agent, $p_i \in \mathbb{R}^2$ is the position vector for agent i, and $u_i \in \mathbb{R}^2$ is the velocity control input to be determined. The goal of this paper is to design a control algorithm u_i for each agent $i, i = 1, \cdots, N$ such that the multi-agent systems can achieve:

(1) Velocity alignment: all agents achieve the same translational velocity

$$\lim_{t\to\infty}[\dot{p}_i(t) - \dot{p}_j(t)] = 0, \forall i, j \in \mathcal{V}. \tag{4}$$

(2) The desired angle rigid formation described by $\mathcal{A}$: the first three agents achieve the desired triangular shape

$$\lim_{t\to\infty} e_i(t) = \lim_{t\to\infty}(\alpha_i(t) - \alpha_i^*) = 0, \forall i = 1, 2, 3, \tag{5}$$

where $\alpha_i^* \in (0, \pi)$ denotes agent i's desired interior angle, and naturally $\alpha_1^* + \alpha_2^* + \alpha_3^* = \pi$.

Each agent from 4 to N achieves the desired two angles

$$\lim_{t\to\infty} e_{i1}(t) = \lim_{t\to\infty}(\alpha_{j_1ij_2}(t) - \alpha^*_{j_1ij_2}) = 0, \tag{6}$$

$$\lim_{t\to\infty} e_{i2}(t) = \lim_{t\to\infty}(\alpha_{j_2ij_3}(t) - \alpha^*_{j_2ij_3}) = 0, \tag{7}$$

where $i = 4, \cdots, N$, $j_1 < i, j_2 < i, j_3 < i$, and $\alpha^*_{j_1ij_2} \in (0, \pi), \alpha^*_{j_2ij_3} \in (0, \pi)$ denote agent i's two desired angles formed with agents $j_1, j_2, j_3 \in \{1, 2, ..., N-1\}$.

3. MAIN RESULTS

In this section, we first introduce the control algorithm design. Then, the angle dynamics of the first three agents and the agents from 4 to N will be given, respectively. Finally, we provide the stability analysis for the closed-loop angle dynamics and velocity alignment dynamics.

3.1 Control algorithm design

In Basiri et al. (2010), by using the bearing measurements, three agents asymptotically achieved a stationary triangular formation shape described by three interior angles $\alpha_i^*, i = 1, 2, 3$. In Basiri et al. (2010), each agent's dynamics are governed by

$$\dot{p}_i = u_i = v_{si}\begin{bmatrix}\cos\beta_i \\ \sin\beta_i\end{bmatrix}, i = 1, ..., 3, \tag{8}$$

where $p_i \in \mathbb{R}^2$ denotes the position of agent i, and $v_{si} \in \mathbb{R}$ is the speed, and the heading angle β_i is defined counterclockwise with respect to agent i's local X-direction and always takes its value from $[0, 2\pi)$. Both v_{si} and β_i are the control inputs to be determined. The control algorithm designed in Basiri et al. (2010) is

$$v_{si} = -k_i(\alpha_i - \alpha_i^*), i = 1, 2, 3, \tag{9}$$

$$\beta_i = \begin{cases}\alpha_i/2 + \min\{\phi_{i(i+1)}, \phi_{i(i-1)}\}, \text{ if } \theta_i \le \pi \\ \alpha_i/2 + \max\{\phi_{i(i+1)}, \phi_{i(i-1)}\}, \text{ if } \theta_i > \pi\end{cases} \tag{10}$$

which physically means that agent i always moves towards the bisector of the interior angle α_i with the speed $|k_i(\alpha_i - \alpha_i^*)|$, where k_i is a positive constant. Actually, when the three agents are not collinear, the control algorithms (9)-(10) can be equivalently written as

$$u_i = -k_i(\alpha_i - \alpha_i^*)\frac{z_{i(i+1)} + z_{i(i-1)}}{\|z_{i(i+1)} + z_{i(i-1)}\|}, \tag{11}$$

where the unit vector $z_{i(i+1)} = \frac{p_{i+1} - p_i}{\|p_{i+1} - p_i\|} = \begin{bmatrix}\cos\phi_{i(i+1)} \\ \sin\phi_{i(i+1)}\end{bmatrix}$ is a function of the bearing $\phi_{i(i+1)}$. In the following analysis, we also term z_{ij} as a bearing or bearing vector since z_{ij} has a unique correspondence to ϕ_{ij} when $p_i \neq p_j$. Then the interior angle α_i can be obtained by $\cos\alpha_i = z^{\mathrm{T}}_{i(i+1)}z_{i(i-1)}$ for $\alpha_i \in (0, \pi)$. For later convenience, we choose a variation on the above law, which preserves the direction of the vector u_i but changes its magnitude. To be specific, the formation stabilization control law is designed as

$$u_i = -k_i(\alpha_i - \alpha_i^*)(z_{i(i+1)} + z_{i(i-1)}). \tag{12}$$

Now, to achieve velocity alignment as well as shape stabilization, and to move beyond just three agents, we first generalize the formation stabilization control law (12) to handle an arbitrary number of agents and then embed within it a virtual velocity variable y_i which is governed by the velocity alignment dynamics. To be specific, we design the angle-based formation control algorithm and velocity alignment dynamics by

$$u_i = -k_i\sum\nolimits_{(j,i,k)\in\mathcal{A}}(\alpha_{jik} - \alpha^*_{jik})(z_{ij} + z_{ik}) + y_i, \tag{13}$$

$$\varepsilon\dot{y}_i = -\sum\nolimits_{j\in\mathcal{N}_i}(y_i - y_j), \tag{14}$$

where $k_i > 0$, ε is a small positive constant, and y_i is an internal state of the system which can be seen as a virtual velocity variable and is governed by single-integrator dynamics.

Now, we present the main result of this paper.

Theorem 1. Consider N agents governed by (3). If Assumptions 1-2 hold, under the control algorithms (13)-(14), the velocity alignment (4) and angle rigid formation (5)-(7) can be achieved locally.

The proof of this theorem is given in the following subsections.

3.2 Angle dynamics of the multi-agent systems

In this subsection, we aim to obtain the angle dynamics of the multi-agent systems under the control algorithm (13). According to the definition of the angle set $\mathcal{A}$, we first analyze the angle dynamics of the first three agents, and then the agents from 4 to N. Differently from Basiri et al. (2010), we use the dot product of two bearings to obtain the angle dynamics, i.e., $\cos\alpha_i = z^{\mathrm{T}}_{i(i+1)}z_{i(i-1)}$ and $\dot{\alpha}_i = \frac{\dot{z}^{\mathrm{T}}_{i(i+1)}z_{i(i-1)} + z^{\mathrm{T}}_{i(i+1)}\dot{z}_{i(i-1)}}{-\sin\alpha_i}$.

According to the Appendix A, one has the following description of the closed-loop angle dynamics of the first three agents

$$\begin{aligned}\dot{e} &= [\dot{\alpha}_1 \ \ \dot{\alpha}_2 \ \ \dot{\alpha}_3]^{\mathrm{T}} = F(e)e + H(e, y) \\ &= \begin{bmatrix}-g_1 & f_{12} & f_{13} \\ f_{21} & -g_2 & f_{23} \\ f_{31} & f_{32} & -g_3\end{bmatrix}\begin{bmatrix}\alpha_1 - \alpha_1^* \\ \alpha_2 - \alpha_2^* \\ \alpha_3 - \alpha_3^*\end{bmatrix} + \begin{bmatrix}h_1 \\ h_2 \\ h_3\end{bmatrix},\end{aligned} \tag{15}$$

where e_i is defined in (5), $l_{ij} = \|p_i - p_j\|$, and $g_i = (\sin\alpha_i)(k_i/l_{i(i+1)} + k_i/l_{i(i-1)})$, $f_{ij} = k_j(\sin\alpha_j)/l_{ij}$, $h_i =$

$\frac{(y_i-y_{i+1})^{\mathrm{T}}[z_{i(i-1)}-z_{i(i+1)}\cos\alpha_i]}{l_{i(i+1)}\sin\alpha_i}-\frac{(y_{i-1}-y_i)^{\mathrm{T}}[z_{i(i+1)}-z_{i(i-1)}\cos\alpha_i]}{l_{i(i-1)}\sin\alpha_i}$.
Since $e_1+e_2+e_3\equiv 0$, one has $\dot{e}_1+\dot{e}_2+\dot{e}_3\equiv 0$ which implies that the dynamics of e_1, e_2 and e_3 are dependent on each other. To analyze the stability of (15), we consider the sub-dynamics of (15)

$$\begin{aligned}\dot{e}_s=\begin{bmatrix}\dot{e}_1\\ \dot{e}_2\end{bmatrix}=&\begin{bmatrix}-(g_1+f_{13}) & f_{12}-f_{13}\\ f_{21}-f_{23} & -(g_2+f_{23})\end{bmatrix}\begin{bmatrix}e_1\\ e_2\end{bmatrix}\\&+\begin{bmatrix}\tilde{w}_{11} & \tilde{w}_{12} & \tilde{w}_{13}\\ \tilde{w}_{21} & \tilde{w}_{22} & \tilde{w}_{23}\end{bmatrix}\begin{bmatrix}y_2-y_1\\ y_3-y_2\\ y_1-y_3\end{bmatrix}\\=&F_1(e_s)e_s+W_1(e_s)Y_1(y_1,y_2,y_3),\end{aligned}\tag{16}$$

where $\tilde{w}_{11}=\frac{(z_{12}\cos\alpha_1-z_{13})^{\mathrm{T}}}{l_{12}\sin\alpha_1}$,$\tilde{w}_{12}=0$, $\tilde{w}_{13}=\frac{(z_{12}-z_{13}\cos\alpha_1)^{\mathrm{T}}}{l_{13}\sin\alpha_1}$, $\tilde{w}_{21}=\frac{(z_{23}-z_{21}\cos\alpha_2)^{\mathrm{T}}}{l_{12}\sin\alpha_2}$, $\tilde{w}_{22}=-\frac{(z_{21}-z_{23}\cos\alpha_2)^{\mathrm{T}}}{l_{23}\sin\alpha_2}$, $\tilde{w}_{23}=0$.

Now, we aim at obtaining the angle dynamics of agents 4 to N. We first consider agent 4, then use induction to obtain the angle dynamics of the remaining agents. For agent 4, (13)-(14) can be written as

$$\begin{aligned}u_4=&-k_{41}(\alpha_{142}-\alpha^*_{142})(z_{41}+z_{42})\\&-k_{42}(\alpha_{243}-\alpha^*_{243})(z_{42}+z_{43})+y_4,\end{aligned}\tag{17}$$

$$\varepsilon\dot{y}_4=-\sum\nolimits_{j\in\mathcal{N}_4}(y_4-y_j),\tag{18}$$

where k_{41} and k_{42} are positive constants. By following a similar analysis in Appendix A, the angle dynamics of e_{41} and e_{42} under the control algorithm (17) can be obtained as follows:

$$\begin{aligned}\dot{e}_4=&[\dot{\alpha}_{142}\ \ \dot{\alpha}_{243}]^{\mathrm{T}}\\=&F_4(e_4)e_4+H_4(e_4)e_s+W_4(e_4)Y_4(y_1,y_2,y_3,y_4)\\=&\begin{bmatrix}-w_1 & r_{12}\\ r_{21} & -w_2\end{bmatrix}\begin{bmatrix}\alpha_{142}-\alpha^*_{142}\\ \alpha_{243}-\alpha^*_{243}\end{bmatrix}+\begin{bmatrix}h_{11} & h_{12}\\ h_{21} & h_{22}\end{bmatrix}\begin{bmatrix}e_1\\ e_2\end{bmatrix}\\&+\begin{bmatrix}w_{11} & w_{12} & w_{13}\\ w_{21} & w_{22} & w_{23}\end{bmatrix}\begin{bmatrix}y_1-y_4\\ y_2-y_4\\ y_3-y_4\end{bmatrix},\end{aligned}\tag{19}$$

where $e_4=[\alpha_{142}-\alpha^*_{142}\ \alpha_{243}-\alpha^*_{243}]^{\mathrm{T}}$, $w_1=(k_{41}/l_{41}+k_{41}/l_{42})(\sin\alpha_{142})$, $w_2=(k_{42}/l_{43}+k_{42}/l_{42})(\sin\alpha_{243})$, $r_{12}=-\frac{k_{42}(\sin\alpha_{142}+\sin\alpha_{143})}{l_{41}}+\frac{k_{42}\sin\alpha_{243}}{l_{42}}$, $r_{21}=-\frac{k_{41}(\sin\alpha_{243}+\sin\alpha_{143})}{l_{43}}+\frac{k_{41}\sin\alpha_{142}}{l_{42}}$, $h_{11}=\frac{k_1z^{\mathrm{T}}_{42}P_{z_{41}}(z_{12}+z_{13})}{l_{41}\sin\alpha_{142}}$, $h_{12}=\frac{k_2z^{\mathrm{T}}_{41}P_{z_{42}}(z_{21}+z_{23})}{l_{42}\sin\alpha_{142}}$, $h_{21}=-k_3\frac{z^{\mathrm{T}}_{42}P_{z_{43}}(z_{31}+z_{32})}{l_{43}\sin\alpha_{243}}$, $h_{22}=k_2\frac{z^{\mathrm{T}}_{43}P_{z_{42}}(z_{21}+z_{23})}{l_{42}\sin\alpha_{243}}-k_3\frac{z^{\mathrm{T}}_{42}P_{z_{43}}(z_{31}+z_{32})}{l_{43}\sin\alpha_{243}}$, $w_{11}=-\frac{z^{\mathrm{T}}_{42}P_{z_{41}}}{l_{41}\sin\alpha_{142}}$, $w_{12}=-\frac{z^{\mathrm{T}}_{41}P_{z_{42}}}{l_{42}\sin\alpha_{142}}$, $w_{13}=0$, $w_{21}=0$,$w_{22}=-\frac{z^{\mathrm{T}}_{43}P_{z_{42}}}{l_{42}\sin\alpha_{243}}$, $w_{23}=-\frac{z^{\mathrm{T}}_{42}P_{z_{43}}}{l_{43}\sin\alpha_{243}}$.

The form of the agent dynamics for agents 5 to N is similar to the form of agent 4. For agent $i, 4<i\le N$ which has two desired angles $\alpha^*_{j_1ij_2},\alpha^*_{j_2ij_3}, j_1<i, j_2<i, j_3<i$ the equations are as follows:

$$\begin{aligned}\dot{e}_i=&[\dot{e}_{i1}\ \ \dot{e}_{i2}]^{\mathrm{T}}=[\dot{\alpha}_{j_1ij_2}\ \ \dot{\alpha}_{j_2ij_3}]^{\mathrm{T}}\\=&F_i(e_i)e_i+H_i(e_i)e_{fi}+W_i(e_i)Y_i(y_{j_1},y_{j_2},y_{j_3},y_i)\\=&\begin{bmatrix}-\bar{w}_1 & \bar{r}_{12}\\ \bar{r}_{21} & -\bar{w}_2\end{bmatrix}\begin{bmatrix}\alpha_{j_1ij_2}-\alpha^*_{j_1ij_2}\\ \alpha_{j_2ij_3}-\alpha^*_{j_2ij_3}\end{bmatrix}+\begin{bmatrix}\bar{h}_{11} & \bar{h}_{12} & \bar{h}_{13}\\ \bar{h}_{21} & \bar{h}_{22} & \bar{h}_{23}\end{bmatrix}\begin{bmatrix}e_{j_1}\\ e_{j_2}\\ e_{j_3}\end{bmatrix}\\&+\begin{bmatrix}\bar{w}_{11} & \bar{w}_{12} & \bar{w}_{13}\\ \bar{w}_{21} & \bar{w}_{22} & \bar{w}_{23}\end{bmatrix}\begin{bmatrix}y_{j_1}-y_i\\ y_{j_2}-y_i\\ y_{j_3}-y_i\end{bmatrix},\end{aligned}\tag{20}$$

where $e_i=\left[\alpha_{j_1ij_2}-\alpha^*_{j_1ij_2}\ \ \alpha_{j_2ij_3}-\alpha^*_{j_2ij_3}\right]^{\mathrm{T}}$, $\bar{w}_1=(k_{i1}/l_{ij_1}+k_{ij_1}/l_{ij_2})(\sin\alpha_{j_1ij_2})$, $\bar{w}_2=(k_{i2}/l_{ij_3}+k_{i2}/l_{ij_2})(\sin\alpha_{j_2ij_3})$, $\bar{r}_{12}=-\frac{k_{i2}(\sin\alpha_{j_1ij_2}+\sin\alpha_{j_1ij_3})}{l_{ij_1}}+\frac{k_{ij_2}\sin\alpha_{j_2ij_3}}{l_{ij_2}}$, $\bar{r}_{21}=-\frac{k_{i1}(\sin\alpha_{j_2ij_3}+\sin\alpha_{j_1ij_3})}{l_{ij_3}}+\frac{k_{i1}\sin\alpha_{j_1ij_2}}{l_{ij_2}}$, $\bar{h}_{11}=k_{j_11}\frac{z^{\mathrm{T}}_{ij_2}P_{z_{ij_1}}(z_{j_1\bar{j}_{11}}+z_{j_1\bar{j}_{12}})}{l_{ij_1}\sin\alpha_{j_1ij_2}}+k_{j_12}\frac{z^{\mathrm{T}}_{ij_2}P_{z_{ij_1}}(z_{j_1\bar{j}_{12}}+z_{j_1\bar{j}_{13}})}{l_{ij_1}\sin\alpha_{j_1ij_2}}$, $\bar{h}_{12}=k_{j_21}\frac{z^{\mathrm{T}}_{ij_1}P_{z_{ij_2}}(z_{j_2\bar{j}_{21}}+z_{j_2\bar{j}_{22}})}{l_{ij_2}\sin\alpha_{j_1ij_2}}+k_{j_22}\frac{z^{\mathrm{T}}_{ij_1}P_{z_{ij_2}}(z_{j_2\bar{j}_{22}}+z_{j_2\bar{j}_{23}})}{l_{ij_2}\sin\alpha_{j_1ij_2}}$, $\bar{h}_{13}=0$, $\bar{h}_{21}=0$, $\bar{h}_{22}=k_{j_21}\frac{z^{\mathrm{T}}_{ij_3}P_{z_{ij_2}}(z_{j_2\bar{j}_{21}}+z_{j_2\bar{j}_{22}})}{l_{ij_2}\sin\alpha_{j_2ij_3}}+k_{j_22}\frac{z^{\mathrm{T}}_{ij_3}P_{z_{ij_2}}(z_{j_2\bar{j}_{22}}+z_{j_2\bar{j}_{23}})}{l_{ij_2}\sin\alpha_{j_2ij_3}}$, $\bar{h}_{23}=k_{j_31}\frac{z^{\mathrm{T}}_{ij_2}P_{z_{ij_3}}(z_{j_3\bar{j}_{31}}+z_{j_3\bar{j}_{32}})}{l_{ij_3}\sin\alpha_{j_2ij_3}}+k_{j_32}\frac{z^{\mathrm{T}}_{ij_2}P_{z_{ij_3}}(z_{j_3\bar{j}_{32}}+z_{j_3\bar{j}_{33}})}{l_{ij_3}\sin\alpha_{j_2ij_3}}$, $\bar{w}_{11}=-\frac{z^{\mathrm{T}}_{ij_2}P_{z_{ij_1}}}{l_{ij_1}\sin\alpha_{j_1ij_2}}$, $\bar{w}_{12}=-\frac{z^{\mathrm{T}}_{ij_1}P_{z_{ij_2}}}{l_{ij_2}\sin\alpha_{j_1ij_2}}$, $\bar{w}_{13}=0$, $\bar{w}_{21}=0$, $\bar{w}_{22}=-\frac{z^{\mathrm{T}}_{ij_3}P_{z_{ij_2}}}{l_{ij_2}\sin\alpha_{j_2ij_3}}$, $\bar{w}_{23}=-\frac{z^{\mathrm{T}}_{ij_2}P_{z_{ij_3}}}{l_{ij_3}\sin\alpha_{j_2ij_3}}$, and $\bar{j}_{11},\bar{j}_{12},\bar{j}_{13}\in\bar{\mathcal{N}}_{j_1}$ are agent j_1's three neighbors. Then, one has the overall compact form of the angle dynamics

$$\begin{aligned}\dot{e}_a=&[\dot{e}_1\ \dot{e}_2\ \dot{e}_{41}\ \dot{e}_{42}\ \cdots\ \dot{e}_{N2}]=A(e_a)e_a+B_a(e_a)Y_a\\=&\begin{bmatrix}F_1(e_s) & 0 & 0 & \cdots & 0\\ H_4(e_4) & F_4(e_4) & 0 & \cdots & 0\\ \cdots & \cdots & \cdots & \cdots & \cdots\\ H_i(e_i) & \cdots & F_i(e_i) & \cdots & 0\\ \cdots & \cdots & \cdots & \cdots & \cdots\\ H_N(e_N) & \cdots & \cdots & \cdots & F_N(e_N)\end{bmatrix}\begin{bmatrix}e_s\\ e_4\\ \cdots\\ e_i\\ \cdots\\ e_N\end{bmatrix}\\&+\begin{bmatrix}W_1(e_s) & 0 & 0 & \cdots & 0\\ 0 & W_4(e_4) & 0 & \cdots & 0\\ \cdots & \cdots & \cdots & \cdots & \cdots\\ \cdots & \cdots & W_i(e_i) & \cdots & \cdots\\ \cdots & \cdots & \cdots & \cdots & \cdots\\ 0 & 0 & 0 & \cdots & W_N(e_N)\end{bmatrix}\begin{bmatrix}Y_1\\ Y_4\\ \cdots\\ Y_i\\ \cdots\\ Y_N\end{bmatrix}.\end{aligned}\tag{21}$$

3.3 Stability analysis

In this subsection, our aim is to establish the local stability of the closed-loop angle dynamics and velocity dynamics. First, we focus on the homogeneous part of the angle dynamics (21), i.e.,

$$\dot{e}_a=A(e_a)e_a.\tag{22}$$

The stability of (22) depends on the property of asymmetric matrix $A(e_a)$. We assume that the initial angle errors $e_a(0)$ are sufficiently small, and then check that $F_1(e_s)|_{e_s=0}$ and $F_i(e_i)|_{e_i=0}, i=4,\cdots,N$ are Hurwitz. By the Hartman-Grobman theorem Wiggins (2003) this will establish that (22) is locally exponentially stable.

For $A_1=F_1(e_s)|_{e_s=0}$, one has

$$\mathrm{tr}(A_1)=-g_1-f_{13}-g_2-f_{23}<0,\tag{23}$$

$$\begin{aligned}\det(A_1)=&(g_1+f_{13})(g_2+f_{23})-(f_{21}-f_{23})(f_{12}-f_{13})\\>&g_1f_{23}+g_2f_{13}+f_{21}f_{13}+f_{12}f_{23}>0,\end{aligned}\tag{24}$$

where we have used the fact that $g_1g_2>f_{21}f_{12}$, and tr() and det() denote the trace and determinant of a square matrix, respectively. Therefore, $F_1(e_s)|_{e_s=0}$ is Hurwitz.

For $A_4=F_4(e_4)|_{e_4=0}$, one has

$$\mathrm{tr}(A_4)=-w_1(\alpha^*)-w_2(\alpha^*)<0,\tag{25}$$

$$\frac{\det(A_4)}{k_1k_2} =$$
$$(\sin\alpha^*_{142}\sin\alpha^*_{243}+\sin^2\alpha^*_{243}+\sin\alpha^*_{243}\sin\alpha^*_{143})\frac{1}{l^*_{42}l^*_{43}}$$
$$+(\sin\alpha^*_{142}\sin\alpha^*_{243}+\sin^2\alpha^*_{142}+\sin\alpha^*_{142}\sin\alpha^*_{143})\frac{1}{l^*_{42}l^*_{41}}$$
$$-\frac{\sin\alpha^*_{142}\sin\alpha^*_{143}+\sin\alpha^*_{143}\sin\alpha^*_{243}+\sin^2\alpha^*_{143}}{l^*_{41}l^*_{43}}, \quad (26)$$

where l^*_{ij} corresponds to the distance between agents i and j in the desired formation shape. Then, if $\det(A_4)>0$, one has that A_4 is Hurwitz. It can be observed that $\det(A_4)>0$ if $l^*_{41}>l^*_{42}$ and $l^*_{43}>l^*_{42}$ hold because

$$l^*_{43}\sin\alpha^*_{142}\sin\alpha^*_{143}>l^*_{42}\sin\alpha^*_{142}\sin\alpha^*_{143}, \quad (27)$$
$$l^*_{41}\sin\alpha^*_{143}\sin\alpha^*_{243}>l^*_{42}\sin\alpha^*_{143}\sin\alpha^*_{243}, \quad (28)$$

and

$$\begin{aligned}\sin^2\alpha^*_{143} =&[\sin\alpha^*_{142}\cos\alpha^*_{243}+\cos\alpha^*_{142}\sin\alpha^*_{243}]^2\\ =&\sin^2\alpha^*_{142}\cos^2\alpha^*_{243}+\cos^2\alpha^*_{142}\sin^2\alpha^*_{243}\\ &+2\sin\alpha^*_{142}\cos\alpha^*_{243}\cos\alpha^*_{142}\sin\alpha^*_{243}, \quad (29)\end{aligned}$$

and

$$l^*_{41}\sin^2\alpha^*_{243}>l^*_{42}\sin^2\alpha^*_{243}\cos^2\alpha^*_{142}, \quad (30)$$
$$l^*_{43}\sin^2\alpha^*_{142}>l^*_{42}\sin^2\alpha^*_{142}\cos^2\alpha^*_{243}, \quad (31)$$
$$\begin{aligned}&l^*_{41}\sin\alpha^*_{142}\sin\alpha^*_{243}+l^*_{43}\sin\alpha^*_{142}\sin\alpha^*_{243}\\ &>2l^*_{42}\sin\alpha^*_{142}\sin\alpha^*_{243}\\ &>2l^*_{42}\sin\alpha^*_{142}\cos\alpha^*_{243}\cos\alpha^*_{142}\sin\alpha^*_{243}. \quad (32)\end{aligned}$$

Therefore, one has that $A_4=F_4(e_4)|_{e_4=0}$ is Hurwitz. Similarly, by using condition $l^*_{ij_1}>l^*_{ij_2}$ and $l^*_{ij_3}>l^*_{ij_2}$, one also has $A_i=F_i(e_i)|_{e_i=0}, i=5,\cdots,N$ are Hurwitz. By using characteristic polynomial to calculate the eigenvalues of $A(e_a)|_{e_a=0}$, one has that if $A(e_a)|_{e_a=0}$ is lower triangular and all its diagonal block matrices are Hurwitz, then $A(e_a)|_{e_a=0}$ is also Hurwitz (Bernstein, 2009, Proposition 5.5.13).

Now, we consider the velocity alignment dynamics (14), which can be written as the compact form

$$\varepsilon\dot{y}=-(\mathcal{L}\otimes I_2)y, \quad (33)$$

where $y=[y_1^{\mathrm{T}},\cdots,y_N^{\mathrm{T}}]^{\mathrm{T}}\in\mathbb{R}^{2N}$, and $\otimes$ denotes the Kronecker product. Following the approach employed in Deghat et al. (2018), we define $P_1\in\mathbb{R}^{2N\times 2N}$ as an orthonormal matrix whose first two rows are $\frac{1^{\mathrm{T}}\otimes I_2}{\sqrt{N}}$ and define $\bar{y}$ as

$$\bar{y}=P_1y. \quad (34)$$

Then, one has the overall dynamics of the multi-agent systems

$$\dot{e}_a=A(e_a)e_a+B_a(e_a)Y_a, \quad (35)$$
$$\varepsilon\dot{\bar{y}}=-P_1(\mathcal{L}\otimes I_2)P_1^{\mathrm{T}}\bar{y}, \quad (36)$$
$$Y_a=(C\otimes I_2)y=(C\otimes I_2)P_1^{\mathrm{T}}\bar{y}, \quad (37)$$

where $C\in\mathbb{R}^{(3N-3)\times 2N}$ and $C1_{2N}=0$. Note that

$$P_1(\mathcal{L}\otimes I_2)P_1^{\mathrm{T}}=\begin{bmatrix}0_{2\times 2} & 0\\ 0 & \hat{\mathcal{L}}\end{bmatrix}, \quad (38)$$

where $\hat{\mathcal{L}}\in\mathbb{R}^{(2N-2)\times(2N-2)}$ is positive definite under Assumption 1. Let $\bar{y}$ be partitioned as $\bar{y}=[y^{o\mathrm{T}}\quad\hat{y}^{\mathrm{T}}]^{\mathrm{T}}$ where $y^{o\mathrm{T}}$ is a 2-vector and $\hat{y}$ is a $2N-2$ vector.

In the following, we use the singular perturbation approach Deghat et al. (2018); Khalil (2002) to obtain the stability of the overall dynamics (36) and the impact of parameter ε on the system convergence rate. Denote $\bar{A}=A(e_a)|_{e_a=0}$. Let Q_2 be an arbitrary positive definite symmetric matrix, since $\bar{A}$ is Hurwitz, there exists a constant and positive definite matrix $P_2\in\mathbb{R}^{(2N-4)\times(2N-4)}$ satisfying $Q_2=-[P_2\bar{A}+\bar{A}^{\mathrm{T}}P_2]$. The angle dynamics (35) can be written as

$$\dot{e}_a=\bar{A}e_a+g(e_a)+B_a(e_a)Y_a, \quad (39)$$

where $g(e_a)=[A(e_a)-\bar{A}]e_a$ satisfies that for any $\gamma>0$, there exists a small $r>0$ such that $\|g(e_a)\|<\gamma\|e_a\|,\forall\|x\|<r$ (Khalil, 2002, Theorem 4.7). Consider the following Lyapunov function

$$V_1=0.5[(1-d)e_a^{\mathrm{T}}P_2e_a+d\hat{y}^{\mathrm{T}}\hat{y}], \quad (40)$$

where $0<d<1$. Taking the time-derivative of (40) yields

$$\begin{aligned}\dot{V}_1=&-(1-d)e_a^{\mathrm{T}}Q_2e_a-\frac{d}{\varepsilon}\hat{y}^{\mathrm{T}}\hat{\mathcal{L}}\hat{y} \quad (41)\\ &+\frac{1-d}{2}e_a^{\mathrm{T}}P_2B_a(e_a)\bar{C}P_1^{\mathrm{T}}\begin{bmatrix}y^o\\ \hat{y}\end{bmatrix}+(1-d)e_a^{\mathrm{T}}P_2g(e_a),\end{aligned}$$

where $\bar{C}=C\otimes I_2$. According to the definition of C and P_1, the first two columns of $\bar{C}P_1^{\mathrm{T}}$ are zero, which implies that

$$\bar{C}P_1^{\mathrm{T}}\begin{bmatrix}y^o\\ \hat{y}\end{bmatrix}=\bar{C}P_1^{\mathrm{T}}\begin{bmatrix}0\\ \hat{y}\end{bmatrix}. \quad (42)$$

Note that $\|P_1^{\mathrm{T}}[0\quad\hat{y}^{\mathrm{T}}]^{\mathrm{T}}\|=\|\hat{y}\|$, and $\|g(e_a)\|<\gamma\|e_a\|$ and $e_a^TP_2B_a(e_a)\bar{C}P_1^{\mathrm{T}}[0\quad\hat{y}^{\mathrm{T}}]^{\mathrm{T}}\le\|e_a\|\|P_2\|\|\bar{B}_a\|\|\bar{C}\|\|\hat{y}\|,\forall\|x\|<r$. Then, one has

$$\dot{V}_1\le-[\|e_a\|\ \|\hat{y}\|]\,Q_3\begin{bmatrix}\|e_a\|\\ \|\hat{y}\|\end{bmatrix}, \quad (43)$$

where

$$Q_3=\begin{bmatrix}(1-d)[\lambda_1(Q_2)-\gamma\|P_2\|] & -\frac{(1-d)\|P_2\|\|\bar{B}_a\|\|\bar{C}\|}{2}\\ -\frac{(1-d)\|P_2\|\|\bar{B}_a\|\|\bar{C}\|}{2} & \frac{d}{\varepsilon}\lambda_1(\hat{\mathcal{L}})\end{bmatrix}.$$

Then, we aim at showing that Q_3 is positive definite such that $\dot{V}_1\le 0$. Since the trace of Q_3 is positive, we only need to show the determinant of Q_3 is positive. Note that $\det(Q_3)>0$ if

$$\frac{d}{1-d}\ge\frac{\varepsilon(\|P_2\|\|\bar{B}_a\|\|\bar{C}\|)^2}{4[\lambda_1(Q_2)-\gamma\|P_2\|]\lambda_1(\hat{\mathcal{L}})}. \quad (44)$$

So for any given $\varepsilon>0$, we can choose d, which might be close to 1 for small values of ε, such that (44) holds. By following a similar analysis to that in Basiri et al. (2010), one can obtain the maximum value of ε to guarantee the stability (which is omitted due to page limitations). In practice, the velocity alignment dynamics should be faster than the stabilization of formation shape, which implies that ε should be sufficiently small.

4. SIMULATION

In this section, we use a numerical simulation to demonstrate the effectiveness of the theoretical results. We consider 4 agents, and their initial states are $p_1(0)=[0,1.2]^T, p_2=[0.3,0]^T, p_3=[\sqrt{3},0]^T$, and $p_4=[0.5,-2]^T$. The desired formation shape is described by 5 angles, the value of which are $[\alpha^*_1,\alpha^*_2,\alpha^*_3,\alpha^*_{142},\alpha^*_{243}]=[60^{\mathrm{o}},60^{\mathrm{o}},60^{\mathrm{o}},72^{\mathrm{o}},62^{\mathrm{o}}]$. Under the control of (14), the formation trajectories and the change of angle errors e_i are given in Fig. 3. It can be seen in Fig. 3 that asymptotically all the agents move in the same direction with the same speed and the angle errors converge asymptotically to zero.

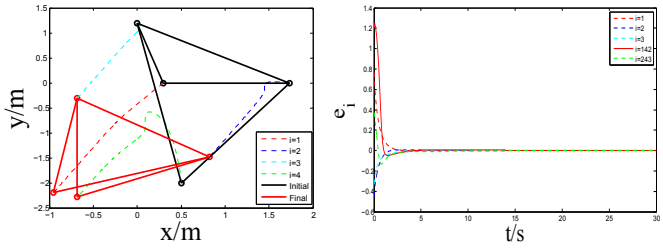

(a) Formation trajectories (b) Change of angle errors

Fig. 3. Simulation results

5. CONCLUSION

This paper has studied the angle-based formation shape control with velocity alignment, which enables all agents to form a desired angle rigid formation and translate with the same velocity simultaneously. The agents' communication topology for the achievement of velocity alignment is described by a connected graph, and the formation shape is described by a set of triple-agent angles. Future work will concentrate on the study of global or almost global convergence, flocking with one leader, and mismatched measurement of angles.

REFERENCES

Ahn, H.S. (2019). *Formation Control: Approaches for Distributed Agents*, volume 205. Springer.

Anderson, B.D.O., Yu, C., Fidan, B., and Hendrickx, J.M. (2008). Rigid graph control architectures for autonomous formations. *IEEE Control Systems Magazine*, 28(6), 48–63.

Basiri, M., Bishop, A.N., and Jensfelt, P. (2010). Distributed control of triangular formations with angle-only constraints. *Systems & Control Letters*, 59(2), 147–154.

Bernstein, D.S. (2009). *Matrix Mathematics:Theory, Facts, and Formulas (Second Edition)*. Princeton University Press.

Chen, L., Cao, M., and Li, C. (2019). Angle rigidity and its usage to stabilize planar formations. *arXiv preprint arXiv:1908.01542*.

Deghat, M., Anderson, B.D.O., and Lin, Z. (2016). Combined flocking and distance-based shape control of multi-agent formations. *IEEE Transactions on Automatic Control*, 61(7), 1824–1837.

Deghat, M., Sun, Z., Nešić, D., and Manzie, C. (2018). Singularly perturbed algorithms for velocity consensus and shape control of single integrator multi-agent systems. *IFAC-PapersOnLine*, 51(23), 200–205.

Jing, G., Zhang, G., Lee, H.W.J., and Wang, L. (2019). Angle-based shape determination theory of planar graphs with application to formation stabilization. *Automatica*, 105, 117–129.

Khalil, H.K. (2002). *Nonlinear systems*, volume 3. Prentice hall Upper Saddle River, NJ.

Krick, L., Broucke, M.E., and Francis, B.A. (2009). Stabilisation of infinitesimally rigid formations of multi-robot networks. *International Journal of control*, 82(3), 423–439.

Oh, K.K. and Ahn, H.S. (2014). Formation control and network localization via orientation alignment. *IEEE Transactions on Automatic Control*, 59(2), 540–545.

Oh, K.K., Park, M.C., and Ahn, H.S. (2015). A survey of multi-agent formation control. *Automatica*, 53, 424–440.

Ren, W. and Beard, R.W. (2008). *Distributed consensus in multi-vehicle cooperative control*. Springer.

Tay, T.S. and Whiteley, W. (1985). Generating isostatic frameworks. *Structural Topology 1985 Núm 11*.

Wiggins, S. (2003). *Introduction to applied nonlinear dynamical systems and chaos*, volume 2. Springer Science & Business Media.

Zhao, S. and Zelazo, D. (2016). Bearing rigidity and almost global bearing-only formation stabilization. *IEEE Transactions on Automatic Control*, 61(5), 1255–1268.

Zhao, S. and Zelazo, D. (2019). Bearing rigidity theory and its applications for control and estimation of network systems: Life beyond distance rigidity. *IEEE Control Systems Magazine*, 39(2), 66–83.

APPENDIX. A

Different from Basiri et al. (2010), we use the dot product of two bearings to obtain the angle dynamics. Take agent 1 as an example,

$$\frac{\mathrm{d}(\cos\alpha_1)}{\mathrm{d}t} = -\sin(\alpha_1)\dot{\alpha}_1 = \frac{\mathrm{d}(z_{12}^{\mathrm{T}} z_{13})}{\mathrm{d}t} = \dot{z}_{12}^{\mathrm{T}} z_{13} + z_{12}^{\mathrm{T}}\dot{z}_{13}. \tag{45}$$

Since for $x \in \mathbb{R}^2, x \neq 0$, $\frac{\mathrm{d}}{\mathrm{d}t}(\frac{x}{\|x\|}) = \frac{P_{x/\|x\|}}{\|x\|}\dot{x}$ where $P_{x/\|x\|} = I_2 - \frac{x}{\|x\|}\frac{x^{\mathrm{T}}}{\|x\|}$ and I_2 is a 2×2 identity matrix, one has

$$\begin{aligned}\dot{z}_{12} =& \frac{P_{z_{12}}}{l_{12}}(u_2 - u_1) = \frac{P_{z_{12}}}{l_{12}}[-k_2(\alpha_2 - \alpha_2^*)(z_{23} + z_{21}) \\ &+ k_1(\alpha_1 - \alpha_1^*)(z_{13} + z_{12}) + y_2 - y_1].\end{aligned}$$

Then, one has

$$\begin{aligned}\dot{z}_{12}^{\mathrm{T}} z_{13} =& \frac{1}{l_{12}}[k_1(\sin^2\alpha_1)(\alpha_1 - \alpha_1^*) - k_2(\sin\alpha_1\sin\alpha_2)\times \\ &(\alpha_2 - \alpha_2^*) + (y_2 - y_1)^{\mathrm{T}} z_{13} - (y_2 - y_1)^{\mathrm{T}} z_{12}\cos\alpha_1].\end{aligned}$$

Similarly, one obtains

$$\begin{aligned}z_{12}^{\mathrm{T}}\dot{z}_{13} =& \frac{1}{l_{13}}[k_1(\sin^2\alpha_1)(\alpha_1 - \alpha_1^*) - k_3(\sin\alpha_1\sin\alpha_3)\times \\ &(\alpha_3 - \alpha_3^*) + (y_3 - y_1)^{\mathrm{T}} z_{12} - (y_3 - y_1)^{\mathrm{T}} z_{13}\cos\alpha_1].\end{aligned}$$

By using (45), one has agent 1's angle dynamics

$$\begin{aligned}\dot{\alpha}_1 =& -(\sin\alpha_1)(\frac{k_1}{l_{12}} + \frac{k_1}{l_{13}})(\alpha_1 - \alpha_1^*) + \frac{k_2\sin\alpha_2}{l_{12}}(\alpha_2 - \alpha_2^*) \\ &+ \frac{k_3\sin\alpha_3}{l_{13}}(\alpha_3 - \alpha_3^*) - \frac{(y_2 - y_1)^{\mathrm{T}}(z_{13} - z_{12}\cos\alpha_1)}{l_{12}\sin\alpha_1} \\ &- \frac{(y_3 - y_1)^{\mathrm{T}}(z_{12} - z_{13}\cos\alpha_1)}{l_{13}\sin\alpha_1}.\end{aligned} \tag{46}$$

Similarly, one can also obtain the angle dynamics of α_2 and α_3

$$\begin{aligned}\dot{\alpha}_2 =& -(\sin\alpha_2)(\frac{k_2}{l_{21}} + \frac{k_2}{l_{23}})(\alpha_2 - \alpha_2^*) + \frac{k_1\sin\alpha_1}{l_{21}}(\alpha_1 - \alpha_1^*) \\ &+ \frac{k_3\sin\alpha_3}{l_{23}}(\alpha_3 - \alpha_3^*) - \frac{(y_1 - y_2)^{\mathrm{T}}(z_{23} - z_{21}\cos\alpha_2)}{l_{12}\sin\alpha_2} \\ &- \frac{(y_3 - y_2)^{\mathrm{T}}(z_{21} - z_{23}\cos\alpha_2)}{l_{23}\sin\alpha_2}.\end{aligned} \tag{47}$$

$$\begin{aligned}\dot{\alpha}_3 =& -(\sin\alpha_3)(\frac{k_3}{l_{31}} + \frac{k_3}{l_{32}})(\alpha_3 - \alpha_3^*) + \frac{k_1\sin\alpha_1}{l_{31}}(\alpha_1 - \alpha_1^*) \\ &+ \frac{k_2\sin\alpha_2}{l_{32}}(\alpha_2 - \alpha_2^*) - \frac{(y_2 - y_3)^{\mathrm{T}}(z_{31} - z_{32}\cos\alpha_3)}{l_{32}\sin\alpha_3} \\ &- \frac{(y_1 - y_3)^{\mathrm{T}}(z_{32} - z_{31}\cos\alpha_3)}{l_{13}\sin\alpha_3}.\end{aligned} \tag{48}$$